Theory of Tunneling Magnetoresistance for Epitaxial Systems

W. H. Butler[1], *Member, IEEE*, X.-G. Zhang[2], S. Vutukuri[1], M. Chshiev[1], and T. C. Schulthess[2]

[1]Center for Materials for Information Technology (MINT), University of Alabama, Tuscaloosa, Al 35487-0209 USA
[2]Computer Science and Mathematics Division, Oak Ridge National Laboratory, Oak Ridge, TN 37831-6164 USA

The tunneling current for electrons tunneling between crystalline ferromagnetic electrodes through an epitaxial crystalline barrier can be calculated from first principles. These calculations show that the wave function symmetry can be exploited to achieve very high tunneling magnetoresistance. For the Fe(100)|MgO(100) |Fe(100) system, the calculated conductance is much higher and its decrease with MgO thickness is much slower than has been estimated using a simple free electron-barrier model.

***Index Terms*—Co, cobalt, Fe, iron, magnesium oxide, magnetoresistance, MgO, symmetry, tunneling.**

I. Introduction

We consider electrical transport between two ferromagnetic electrodes separated by an insulating barrier. It is observed experimentally that the electrical resistance of the barrier depends on the relative alignment of the magnetic moments of the electrodes. Denoting the resistance for parallel alignment by R_P and that for antiparallel alignment by R_A, the tunneling magnetoresistance (TMR) may be defined as

$$\mathrm{TMR} = \frac{R_A - R_P}{R_P}. \tag{1}$$

Until recently, our understanding of the TMR phenomenon was based on a formula due to Julliere [1] which related the TMR to the "polarization" of the ferromagnetic electrodes, P. Thus, Julliere's formula would predict that

$$\mathrm{TMR} = \frac{2P_1P_2}{1 - P_1P_2} \tag{2}$$

where P_1 and P_2 are the "polarizations" of the two electrodes. It has long been known [2], [3] that this model has limitations, among which is that it has never been entirely clear how the polarization, P, should be defined.

In this paper, we discuss systems in which very large TMR can be obtained using simple ferromagnetic electrodes such as Co, Fe, and CoFe together with epitaxial crystalline tunneling barriers. The TMR's calculated for these systems (as well as measured experimentally) are much too high to be consistent with the Julliere model using any reasonable definition of electrode polarization.

II. Effects of Wave Function Symmetry on Tunneling Probability

A. Wave Function Symmetry

Consider a system consisting of two semi-infinite ferromagnetic electrodes separated by an insulating barrier. We assume that the insulating barrier fits epitaxially to the electrodes and that two-dimensional (2-D) order parallel to the interfaces between the barrier and the electrodes is maintained. Such systems may be realized approximately experimentally. One example system is Fe(100) electrodes and MgO(100) for the insulating barrier [4], [5]. GaAs(100) and ZnSe(100) and Ge(100) also have lattice parameters that allow a good epitaxial relationship [6]. It is well known that in systems that maintain 2-D periodicity, the component of the electron quasi-momentum transverse to the interface is conserved as the electron traverses the interface. Often, as for example in the cases mentioned above, the wave function symmetry is also preserved. Fig. 1 shows some of the wave function symmetries commonly observed in fcc and bcc transition metals. For Fe in the (100) direction at the Fermi energy, for example, there are Bloch states with symmetries Δ_1, Δ_5, and Δ_2' for the majority and Δ_2, Δ_5, and Δ_2' for the minority.

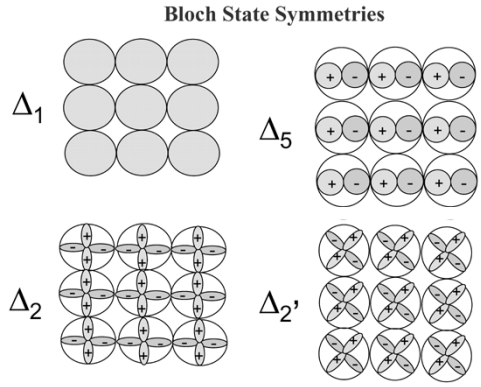

Fig. 1. Some possible symmetries for Bloch states propagating in the 100 direction. The "+" and "−" symbols indicate the sign of the wave function.

B. Spin-Filter Effect From Wave Function Symmetry

This conservation of wave function symmetry allows for a spin filtering effect. Electrons tunnel through the barrier as evanescent Bloch states which match the symmetry of the incident Bloch states in the electrode [7]. Typically, as in the systems mentioned in the previous paragraph, the most slowly decaying evanescent Bloch state in the barrier is the one with highest symmetry. This is illustrated for MgO in Fig. 2. Here, we plot k^2 (where k is the Bloch state quasi-momentum) as

Digital Object Identifier 10.1109/TMAG.2005.854763

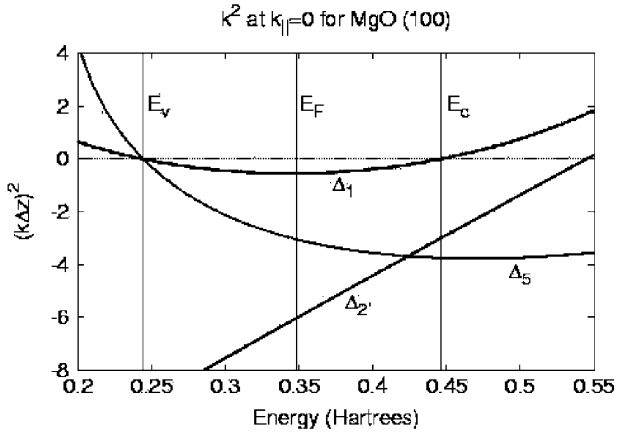

Fig. 2. Bloch states of different symmetry decay at different rates within the insulating barrier.

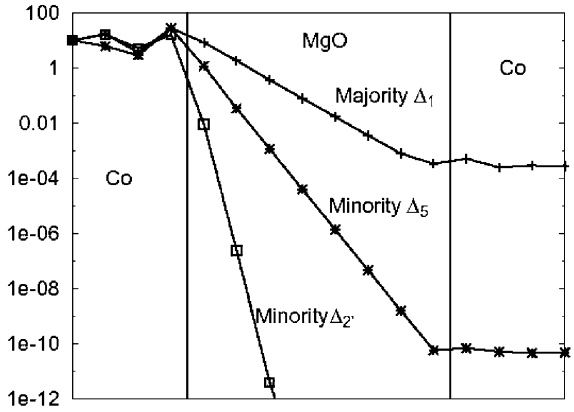

Fig. 3. Bloch state density for bcc Co electrodes on either side of an MgO barrier eight atomic layers thick as a function of layer number for parallel alignment of the moments in the electrodes. The symbols indicate successive atomic layers. The boundary conditions are for single Bloch states incident from the left.

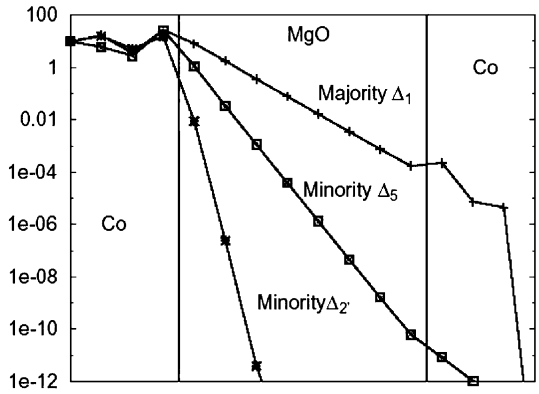

Fig. 4. Bloch state density for bcc Co electrodes on either side of an MgO tunneling barrier as a function of the layer number for antiparallel alignment of the electrode moments. Symbols indicate successive atomic layers.

a function of Energy for Bloch states traveling in the (100) direction. E_v labels the top of the valence band and E_c is the bottom of the conduction band. The conduction band is a Δ_1 state and the valence bands are a combination of Δ_1 and Δ_5 states. The Δ_1 state continues through the gap as an evanescent state with a relatively small (negative) value of k^2.

If one can find a ferromagnetic electrode system which has a state with this high symmetry at the Fermi energy for one spin channel, but not for the other, then the spin-filtering effect can occur. When the magnetic moments of the electrodes are aligned, (e.g., Fig. 3) the conductance of the spin channel with the high-symmetry Bloch state is high while that of the other channel is relatively much lower. The contrast in the channels can be quite large because both conductances will decrease exponentially with thickness, but with different rates.

When the magnetic moments of the two electrodes are anti-aligned, the conductance of both channels is low. In one channel, there will be no high symmetry state so its conductance will be low. In the other channel, the high-symmetry state that is injected from one of the electrodes and traverses the barrier with slow decay will be reflected at the barrier-electrode interface of the other electrode because that electrode (by assumption) does not support propagation of the high-symmetry state.

In addition to Fe(100), bcc Co(100) and CsCl structure FeCo(100) have the property described above of a high symmetry Δ_1 state at $k_{||} = 0$ for majority, but not for minority. The latter two systems (bcc Co and FeCo) are particularly well suited to illustrate this effect because they have only a single majority state along (100) and that state is Δ_1. The symmetry based spin-filtering effect is most effective for $k_{||=0}$, i.e., for those electrons traveling perpendicular to the interfaces.

C. First-Principles Calculations of Spin-Dependent Tunneling

For devices such as tunnel junctions in which the electron transport is perpendicular to the layers it is convenient to use the Landauer–Büuttiker approach [8], [9]. In the simplest version of this approach as applied to tunneling, one imagines leads on either side of a barrier. If the leads are infinite and periodic in the direction normal to the barrier, one can classify the quantum states according to their transverse normal modes. Each of the propagating transverse normal modes at the Fermi energy acts as a possible conduction channel. The conductance is then given by the sum over these conduction channels of one of the leads of the probability that it will be transmitted. For the case of a system with 2-D periodicity transverse to the direction of propagation, the Landauer formula can be written as

$$G = \frac{e^2}{h} \sum_{k_{||},i,j} T(k_{||}, i, j) \tag{1}$$

where, $k_{||}$ is the transverse quasi-momentum of one of the leads and i and j label Bloch states on opposite sides of the barrier. $T(k_{||}, i, j)$ is the probability that Bloch state i on one side of the barrier will be transmitted in to Bloch state j on the other side.

This approach was used to calculate the conductance for aligned and anti-aligned matched electrodes of Fe(100), Co(100), and FeCo(100) separated by an epitaxial MgO barrier. Resistance ratios $(R_A)/R_P)$ of 54, 130, and 340 for these three cases respectively were obtained when the thickness of the MgO was 8 atomic layers [10]. These calculations assumed perfectly ordered systems.

D. Effects of Interfacial Wave Function Overlap

Another important factor that contributes to the high TMR in these systems is that the high-symmetry, majority-spin Bloch

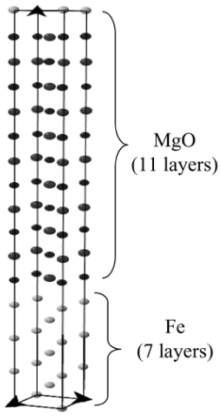

Fig. 5. Supercell used to demonstrate decay of wavefunction within barrier.

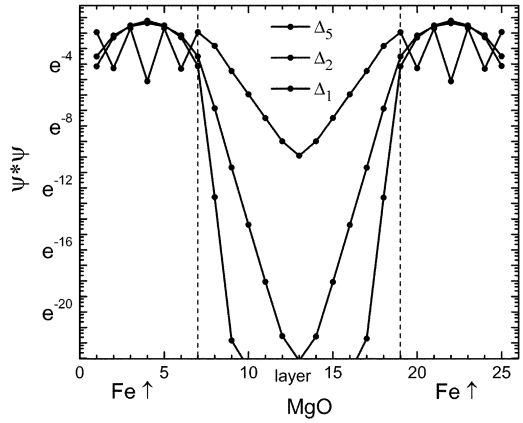

Fig. 6. Absolute square of Δ_1, Δ_5, and Δ_2 wave functions in an Fe-MgO supercell. Because of the $\pi/4$ rotation of the cube axes between Fe and MgO, states that have Δ_2' symmetry in Fe are Δ_2 in MgO and vice versa. Here, states are labeled by their symmetry in the MgO.

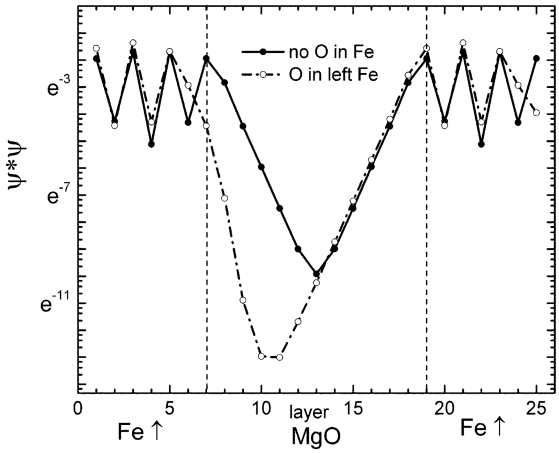

Fig. 7. State density, $\psi^*\psi$ for Fe-MgO-Fe majority with and without O in the final Fe layer on the left side.

state responsible for the large TMR has a strong overlap between the interfacial Fe or Co atoms and oxygen atoms situated directly above. If this strong overlap is destroyed, for example by introducing oxygen atoms into the interfacial Fe layer [11], the majority conductance and the TMR is drastically reduced. This latter effect can be demonstrated using the Landauer approach, as was done for example, in [11] in which the effect of oxygen atoms in the interfacial Fe layer of an Fe(100)|MgO(100)|Fe(100) tunnel junction dramatically reduces the majority conductance and the TMR. This effect has also been emphasized by Tsymbal [12], [13].

Here, we demonstrate the effect using a simple band structure calculation for an Fe|MgO|Fe supercell shown in Fig. 5. The supercell has 11 MgO atomic layers and 7 Fe atomic layers. The electronic structure was calculated using a popular plane wave-based code [14]–[17] and the states near the Fermi energy were examined. The state density, $\psi^*\psi$ for the majority spin, Δ_1, Δ_2', and Δ_5 states for each atomic layer are shown in Fig. 6. Just as in Fig. 4, there is a huge difference in the way wave functions that live primarily on the Fe decay into the MgO. The Δ_1 states decay relatively slowly, the Δ_5 states more rapidly and the $\Delta_{2'}$ states most rapidly.

Fig. 7 illustrates the effect on the Δ_1 state of the overlap between the wave function on the interfacial Fe and the oxygen atom directly above it (assuming the layers are stacked vertically as in Fig. 5) in the interfacial MgO layer. In this calculation, the interfacial Fe layer on the left side contained additional O atoms at the interstitial position. The additional O atoms at the interface destroy the overlap between the states on the Fe and on the O in the MgO, dramatically increasing the rate of decay of the state density into the MgO from that side.

E. Comparison With Experiment

Recent reports of very high TMR in systems similar to those described here [18], [19] lend support to this theory of high TMR for systems with crystalline barriers. Our calculated conductance for the parallel configuration in Fe|MgO |Fe agrees reasonably well with that measured in [18]. For example, our calculated value of RA for eight layers of MgO is 320 $\Omega(\mu\text{m})^2$ whereas the measured value is approximately 310 $\Omega(\mu\text{m})^2$. Although this level of agreement is probably fortuitous, it is clear that our calculations are not off by orders of magnitude and, in fact, appear to be surprisingly close to experiment given the exponential dependencies on thickness and on the details of the electronic structure.

There has been much interest in the apparent relatively low energy barrier deduced from the dependence of the conductance on the barrier thickness. If one deduces a barrier height from the free electron expression for the rate of increase in RA, one obtains an effective energy barrier of approximately 0.4 eV. This is more than an order of magnitude less than the optical energy gap of MgO. A more accurate estimate of the effective energy barrier, however, should take into account the effective mass of the valence and conduction electrons and the fact that electron tunneling through MgO is quite different from tunneling through a simple barrier. We have already pointed out that electrons of different symmetry decay at vastly different rates and therefore see vastly different effective energy barriers. Using the calculated energy bands, we estimate the effective mass of the highly dispersing Δ_1 conduction and valence band states that give rise to the Δ_1 evanescent ban to be approximately 0.37 m_e. In addition, it is clear from Fig. 1 that low bias

tunneling will involve both holes and electrons. It should be clear, therefore, that the estimates of the gap based on the free electron model should not be expected to be even approximately accurate.

The measured thickness dependence of the parallel RA is $\mathrm{RA} = R_0 A \exp(-kt)$, where t is the MgO thickness and $k \approx 6.5/\mathrm{nm}$ [18]. The calculated value of k varies somewhat depending on the details of the calculations, but our current best estimate, based on the decay rate of the Δ_1 evanescent state is $k \approx 5.6/\mathrm{nm}$. It should be expected that we slightly underestimate the decay rate, because DFT based electronic structure calculations underestimate energy gaps. Our calculated gap is approximately 5.5 eV whereas the experimental gap is approximately 7.5 eV.

The measured resistance of the antiparallel configuration is lower than predicted by our calculations due in part to thermal, chemical, and structural disorder which allows conductance by states that would be blocked in a perfectly ordered system. It should be noted that the primary effect of thermal disorder is to significantly increase the antiparallel conductance while the parallel conductance is much less affected. This is in agreement with our model of symmetry-blocked conductance of the antiparallel channels.

We speculate that the reason the experimental rate of decrease of conductance with thickness is approximately the same for antiparallel as for parallel alignment of the moments over the thickness regime measured (>1 nm) is that disorder-generated state density with Δ_1 symmetry (and slow decay) dominates the conductance after the more rapidly decaying evanescent states have decayed away.

ACKNOWLEDGMENT

This work was supported by INSIC-EHDR, DARPA, ONR, and by NSF through Grant DMR0213985 and Grant SA4130-10092PG/82939.

REFERENCES

[1] M. Julliere, *Phys. Lett.*, vol. A54, p. 225, 1975.
[2] J. M. MacLaren, X.-G. Zhang, and W. H. Butler, *Phys. Rev. B*, vol. 56, p. 11 287, 1997.
[3] W. H. Butler, X.-G. Zhang, and X.-G. Zhang, *J. Phys.: Condens. Matter*, vol. 15, pp. R1603–R1639, 2003.
[4] W. H. Butler, X.-G. Zhang, T. C. Schulthess, and J. M. MacLaren, *Phys. Rev. B*, vol. 63, p. 054 416, 2001.
[5] J. Mathon, A. Umerski, and A. Umerski, *Phys. Rev. B*, vol. 63, p. 220 403, 2001.
[6] J. M. MacLaren, X.-G. Zhang, W. H. Butler, and X. Wang, *Phys. Rev. B*, vol. 59, p. 5470, 1999.
[7] P. Mavropoulos, N. Papanikolaou, N. Papanikolaou, and P. H. Dederichs, *Phys. Rev. Lett.*, vol. 85, p. 1088, 2000.
[8] R. Landauer, *IBM J. Res. Develop.*, vol. 1, p. 223, 1957.
[9] M. Büttiker, *IBM J. Res. Develop.*, vol. 32, p. 317, 1988.
[10] X.-G. Zhang and W. H. Butler, *Phys. Rev. B*, vol. 70, p. 172 407, 2004.
[11] X.-G. Zhang, W. H. Butler, and A. Bandyopadhyay, *Phys. Rev. B*, vol. 68, p. 092 402, 2003.
[12] E. Y. Tsymbal, O. N. Mryasov, and P. R. LeClair, *J. Phys., Condens. Matter*, vol. 15, pp. R109–R142, 2003.
[13] E. Y. Tsymbal, *Proc. 49th Conf. Magnetism and Magnetic Materials, Invited Presentation*.
[14] G. Kresse and J. Hafner, *Phys. Rev. B*, vol. 47, p. 558, 1993.
[15] G. Kresse, J. Hafner, and J. Hafner, *Phys. Rev. B*, vol. 49, p. 14 251, 1994.
[16] G. Kresse and J. Furthmüller, *Comput. Mat. Sci.*, vol. 6, p. 15, 1996.
[17] G. Kresse and J. Furthmüller, *Phys. Rev. B*, vol. 54, p. 11 169, 1996.
[18] S. Yuasa, T. Nagahama, A. Fukushima, A. Fukushima, Y. Suzuki, and K. Ando, *Nature Mat.*, vol. 3, p. 868, 2004.
[19] S. S. P. Parkin, C. Kaiser, A. Panchula, P. M. Rice, B. Hughes, M. Samant, and S.-H. Yang, *Nature Mat.*, vol. 3, p. 862, 2004.

Manuscript received February 7, 2005.